

# Geoscience Laser Altimeter System (GLAS)

Algorithm Theoretical Basis Document  
Version 1.0

## OCEAN TIDAL LOADING CORRECTIONS

Prepared by:

Donghui Yi  
Raytheon ITSS  
Oceans and Ice Branch, Code 971  
NASA Goddard Space Flight Center  
Greenbelt MD 20771

Jean-Bernard Minster  
Institute of Geophysics and Planetary Physics  
Scripps Institution of Oceanography  
La Jolla CA 92093-0225

Charles Bentley  
Geophysical and Polar Research Center  
University of Wisconsin  
Madison, WI,

February 1999

## 1. Introduction

The vertical displacement caused by the ocean tidal loading is of the order of several tens of millimeters in polar regions. This is important for the GLAS project since it requires centimeter-level accuracy in surface elevation change detection. Applying the ocean tidal loading correction will improve the accuracy of satellite altimeter measured surface elevation over polar regions, especially in the coastal areas. Conversely, assimilation of the altimetry measurements will improve the tidal models at high latitudes.

## 2. Background

If melted, Antarctic and Greenland ice sheets would produce a 72-meter rise in sea level (Oerlemans, 1993). For this factor alone, we need to understand how Antarctica and Greenland will react to the current climate change. In the present century, sea-level rose at an average rate of 1.0-2.0 mm yr<sup>-1</sup> (Warrick, 1993). Part of the sea level rise can be explained by ocean thermal expansion and the melting of glaciers/small ice caps and, perhaps, net mass loss to the Greenland ice sheet. The annual snow fall on the grounded Antarctic ice is equivalent to about 5 mm yr<sup>-1</sup> of global sea level change (Jacobs, 1992), so yearly variation of snowfall on the Antarctic ice sheet can have a measurable effect on sea level. Without independent knowledge of the contribution of the Antarctic ice sheet, there remains a major uncertainty in understanding sea level change (Warrick and Oerlemans, 1990). To fix ideas, assuming that half of the sea-level rise, i.e. 0.5-1.0 mm yr<sup>-1</sup>, comes from a mass loss to the Antarctic ice sheet, then the mean elevation of Antarctica would need to drop at a rate of about 15-30 mm yr<sup>-1</sup>. This estimate ignores the potential contributions of other phenomena, such as post-glacial rebound.

Satellite altimeters can be used to monitor the volume of the polar ice sheets. Substantial progress in studying polar mass balance has been sustained by the use of satellite radar altimeters (Brenner *et al*, 1983, Zwally *et al*, 1989, Zwally, 1989, Partington *et al*, 1991, Bentley and Sheehan, 1992, Lingle *et al*, 1994, Yi *et al*, 1997). However the precision of the satellite radar altimeters is limited by surface slope because of the large radar footprint (Brenner *et al*, 1983), imperfect understanding of the microwave penetration to the subsnow surface (Ridley and Partington, 1988, Yi and Bentley, 1997), and inadequate accuracy of satellite orbits (Haines *et al*, 1994). The Geoscience Laser Altimeter System (GLAS) (Schutz, 1995), designed mainly for measuring polar ice sheets, has a much smaller footprint of about 70 meter which will reduce the surface slope effect and benefits from an on board GPS which will give an orbit accuracy of  $\pm 50$  mm.

Ocean tides and solid earth tides have been taken into account in processing the satellite radar altimetry data (Zwally *et al*, 1990). However, the smaller vertical displacement caused by the ocean tidal loading has heretofore not been taken into account. This is no surprise since the precision of satellite radar altimeters over land is of the order of several tens of centimeters while the vertical displacement load tide is of the order of several tens of millimeters even along the coast. Ocean loading effects only become important when the surface elevation measurements require centimeter-level precision. To determine accurately the surface elevation and surface ele-

variation change, it is important to estimate the ocean tidal loading effects and apply an ocean tidal loading correction to the surface elevation measurement.

### 3. Ocean tidal loading

Various methods have been used to compute tidal loading. *Baker* (1985) lists five of them: (1) the spherical harmonic expansion method; (2) the polygon method; (3) the template method; (4) the spherical disc method; and (5) the Green's function method. In this ATBD, the tidal loading is computed by the Green's function method (*Farrell*, 1972). *Agnew* (1996) produced a software package which makes it is easy to calculate tidal loading at a given point by using the Green's function and an ocean tide model. In *Agnew's* package, the ocean load tide  $L$  is given by

$$L(\theta', \lambda') = \int_0^{2\pi} \left( \int_0^\pi \rho H(\theta, \lambda) G_L(\Delta) S_L(\alpha) a^2 \sin(\theta) d\theta \right) d\lambda \quad (1)$$

where  $\Delta$  is the distance,  $\alpha$  is the azimuth of the point with geographical coordinates  $(\theta, \lambda)$  relative to the place of observation, which is at  $(\theta', \lambda')$ ;  $H$  is the tidal height at  $(\theta, \lambda)$ ,  $\rho$  is ocean water density, and  $a$  is the radius of the earth.  $G_L$  is the mass loading Green's function and  $S_L$  is the combination of trigonometric functions needed to compute a vector or tensor load. The Green functions used are obtained from *Farrell* (1972). There are numerous global tide models available: for example, the Schwiderski model (*Schwiderski*, 1980), the CSR 3.0 model (*Eanes*, 1994), the TPXO.2 model (*Egbert et al*, 1994), and the FES95.2 model (*Le Provost et al*, 1994, 1995). For present purposes, any one of these models can be used with acceptable results.

### 4. Algorithm Description

The displacement component at a location at a time  $t$  is given by (*McCarthy*, 1992)

$$\Delta c = \sum_j f_j A_j \cos(\omega_j t + \chi_j + \mu_j - \Phi_j) \quad (2)$$

where  $f_j$  and  $\mu_j$  depend on the longitude of the lunar node,  $A_j$  and  $\Phi_j$  are the amplitude and phase for each displacement component,  $\omega_j$  is the frequency of tide  $j$  and  $\chi_j$  is the astronomical argument at  $t = 0$ . The three components of displacement (vertical, east-west, north-south) can be calculated by the above equation, but here we are only interested in the vertical displacement.  $\chi_j$  is calculated using the program ARG described by *McCarthy* (1992).  $f_j$  and  $\mu_j$  are calculated by the following relations for the eight largest constituents, which together account for over 90% of the tidal signal (*Doodson*, 1928):

$$f_{m2} = 1.000 - 0.037 \cos(N)$$

$$f_{s2} = 1.0$$

$$f_{n2} = 1.000 - 0.037 \cos(N)$$

$$f_{k2} = 1.024 + 0.286 \cos(N) + 0.008 \cos(2N)$$

$$f_{k1} = 1.006 + 0.115 \cos(N) - 0.009 \cos(2N)$$

$$f_{o1} = 1.009 + 0.187 \cos(N) - 0.015 \cos(2N)$$

$$f_{p1} = 1.0$$

$$f_{q1} = 1.009 + 0.187 \cos(N) - 0.015 \cos(2N)$$

$$\mu_{m2} = -2.1^\circ \sin(N)$$

$$\mu_{s2} = 0.0^\circ$$

$$\mu_{n2} = -2.1^\circ \sin(N)$$

$$\mu_{k2} = -17.7^\circ \sin(N) + 0.7^\circ \sin(2N)$$

$$\mu_{k1} = -8.9^\circ \sin(N) + 0.7^\circ \sin(2N)$$

$$\mu_{o1} = 10.8^\circ \sin(N) - 1.3^\circ \sin(2N) + 0.2^\circ \sin(3N)$$

$$\mu_{p1} = 0.0^\circ$$

$$\mu_{q1} = 10.8^\circ \sin(N) - 1.3^\circ \sin(2N) + 0.2^\circ \sin(3N)$$

$$N = (259.16^\circ - 19.3282^\circ (\text{year}-1900) - 0.0530^\circ (\text{day} + \text{leapyear}))$$

Since the calculation of the amplitude and phase of a tidal constituent is relatively time consuming, an interpolation method on a gridded set of pre-calculated results is used instead. The load tide varies smoothly, so it can be interpolated in space and time with negligible error. We calculate the tidal loading at a point (x, y) by first determining its value at the four nearest neighbors in the grid, interpolating the tidal values at the grid points for the appropriate time. Then we use bilinear spatial interpolation (e.g. *Press et al.*, 1992) to compute the appropriate amplitude and phase of each tidal component at (x, y). Finally, we combine components using Equation 2. "

At each gridded point, the amplitudes and phase of the tidal constituents can be calculated beforehand. Our algorithm is based on the pre- calculation of tides on a 1° by 1° grid globally, (this can be performed on a HP-735 workstation of the GLAS Science Computing Facility, using the software described above with no attempt at streamlining the procedure or optimizing the software). When the pre-calculated results are stored on disk, a million points along a ground track, or about 5 orbits, can be calculated in 7 minutes through bilinear interpolation. "

Figure 1 shows a grid block for the interpolation. The tidal loading L at point (x, y) is calculated by,

$$L(x, y) = (1-c_1)(1-c_2)L(x_1, y_1) + c_1(1-c_2)L(x_2, y_1) + c_1c_2L(x_2, y_2) + (1-c_1)c_2L(x_1, y_2)$$

$$c_1 = (x-x_1)/(x_2-x_1)$$

$$c_2 = (y-y_1)/(y_2-y_1)$$

## A Grid Block

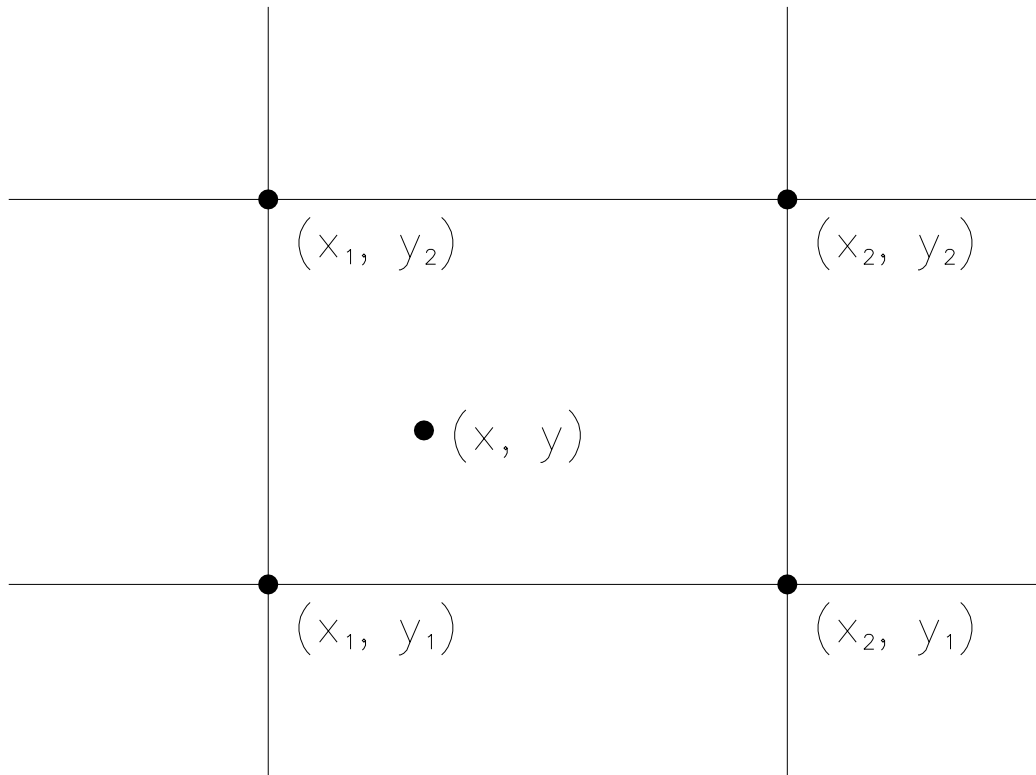


**Figure 1:** Geometry and notation for bilinear interpolation of ocean load tides.

Since the load tide varies smoothly, it can be interpolated in space and time with negligible error. This justifies our approach of tabulating load tide amplitudes and phases on a  $1^\circ \times 1^\circ$  geographical grid. Then, to estimate tidal-loading displacements at any given time and any given point within Antarctica we use bilinear interpolation (e.g. *Press et al.*, 1992) to compute the appropriate amplitude and phase at that location, and use Equation 2. As a check, we compare calculated and interpolated values for a 180-day time series sampled at hourly intervals, starting January 1, 2001, at three locations:  $(66.6617^\circ\text{S}, 140.0014^\circ\text{E})$ ,  $(70.5^\circ\text{S}, 135.5^\circ\text{E})$ , and  $(70.5^\circ\text{S}, 45.5^\circ\text{E})$ . The first point is near the coast, the other two are inland. The standard deviations of the residuals between calculated and interpolated values are 0.35 mm, 0.05 mm, and 0.03 mm, respectively. That is more than accurate enough for correcting the measurements to be made by GLAS. In view of these results, it is clear that calculation of the tides at grid nodes need only be performed once during the time taken by the spacecraft to traverse the grid cell. This indicates that

an effective strategy is to compute the corrections only at a relatively sparse set of points —say, every 15 seconds, that is every 600 shots, or every degree along track— and to interpolate using the shot count as the independent variable along track. This approach will work for any tidal correction, the only caveat being that the transitions from ocean to land environments and *vice versa* must be accounted for by keeping track of the intersections of the ground track with a sufficiently accurate map of the coastlines.

## 5. Discussion

We accounted in Equation 2 for the eight major tidal constituents (four semidiurnal waves:  $m_2$ ,  $n_2$ ,  $s_2$ ,  $k_2$ , and four diurnal waves:  $k_1$ ,  $o_1$ ,  $p_1$ ,  $q_1$ ) that contribute most to tidal loading. We used the tide model FES95.2 to calculate the amplitude and phase of  $m_2$ ,  $n_2$ ,  $s_2$ ,  $k_2$ ,  $k_1$ ,  $o_1$ ,  $q_1$ . TPXO.2 was used to calculate the amplitude and phase of  $p_1$ . We selected FES95.2 mainly because it is the only readily available global ocean-tide model that includes the regions under the Ross, Filchner, and Ronne Ice Shelves around Antarctica, regions which are of major concern to the GLAS project.

### Vertical Displacement (mm)

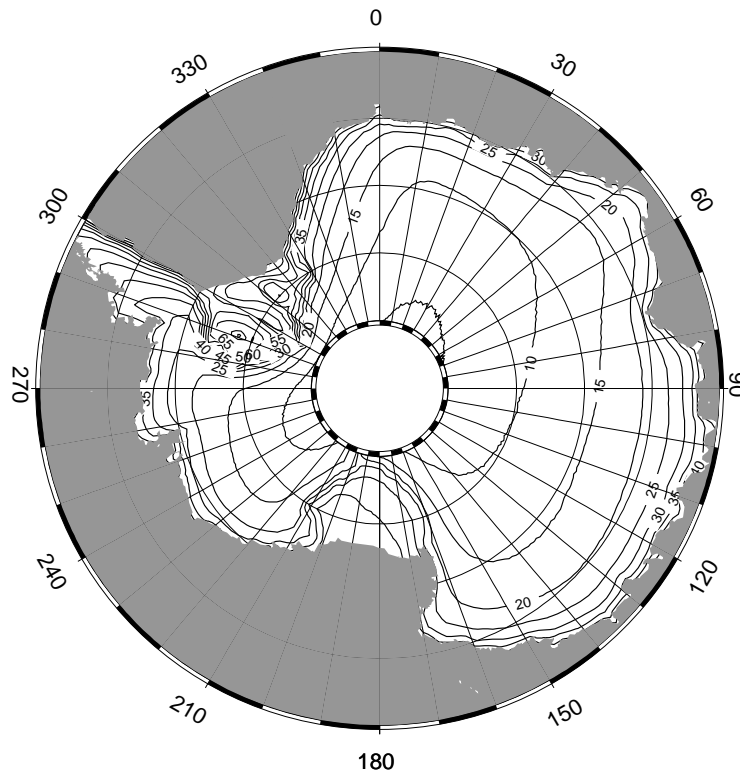


**Figure 2:** Contour map of maximum vertical displacement due to ocean tidal loading over Antarctica.

As a validation of this approach, we compare the vertical displacement computed here to that obtained using amplitude and phase calculated by *McCarthy* (1992) following *Scherneck*

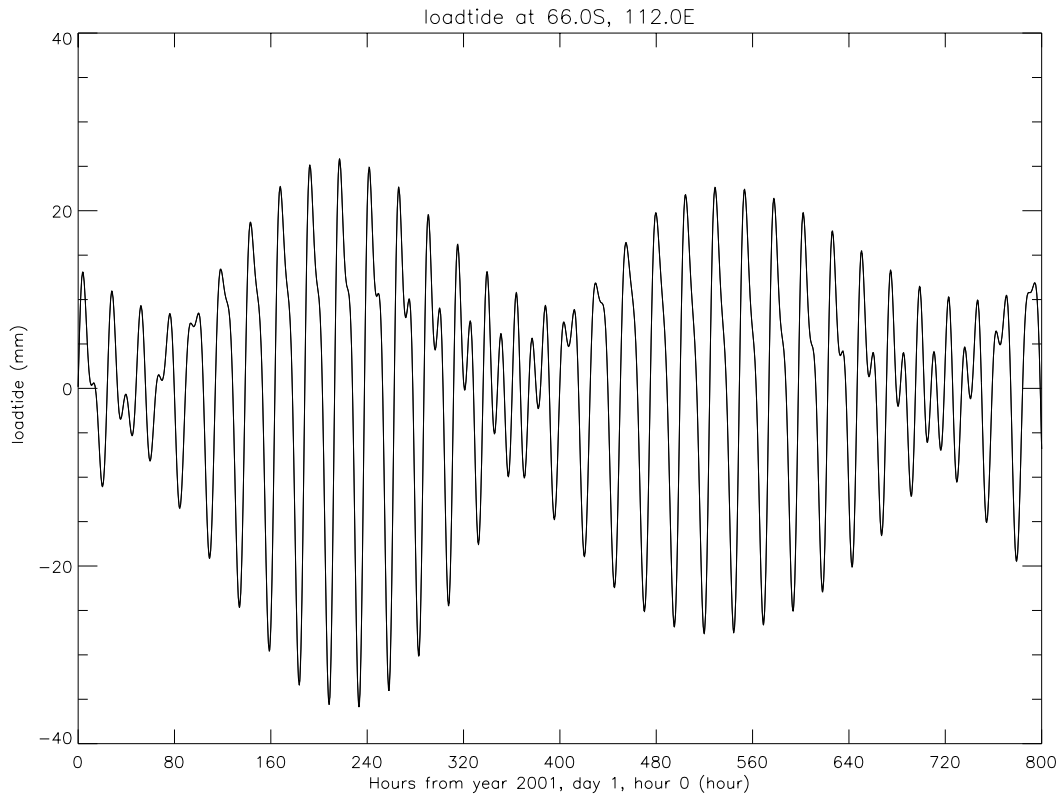


**Figure 3:** Comparison of load tide time series calculated at 1 hour intervals and at 12 minute intervals. This shows that temporal interpolation is justified.

(1991). At a test point ( $66.6617^{\circ}\text{S}$ ,  $140.0014^{\circ}\text{E}$ ) in Antarctica, for a 180-day period starting from January 1, 2001, the difference between the two calculations is less than  $\pm 1.6$  mm. McCarthy's results are estimated to be accurate at the  $\pm 3$  mm level (McCarthy, 1992). Since we used a more recent, presumably improved tide model, we can assume that the accuracy of our calculation is at least as good.

The results show that the vertical tidal loading displacements are typically several centimeters over Antarctica. As expected, the amplitudes are higher along the coast and lower inland. The distribution of the *maximum* possible load tide over Antarctica (the sum of vertical displacements amplitude of eight tide constituents, which is what might be expected if all constituents ever happen to be in phase) is shown in Figure 2. It reaches a maximum value over Antarctica which exceeds 40 mm.

In practice, one sees the largest amplitudes when most of the constituents are in phase. For example at ( $66^{\circ}\text{S}$ ,  $100^{\circ}\text{E}$ ) the maximum amplitude is about 40 mm, but the total range of the displacement time series reaches only about 60 mm in the first ten years of the 21st century, not 80 mm. Figure 3 and Figure 4 are two examples showing the spatial and temporal variations of tidal loading. In Figure 3, two load tide time series are plotted. One is calculated at 1 hour intervals and the other at 0.2 hour intervals. They are indistinguishable, which demonstrates that temporal interpolation is fully justified.

Similarly, in Figure 4, there are two lines plotted: tidal loads calculated every degree and

every half degree of longitude, respectively, at latitude 70degS. Again, the two cannot be distinguished.. For a time series of 180 days starting from January 1, 2001, on one hour intervals, the standard deviation of the differences between the directly calculated value and the bilinear interpolated value are 0.35 mm, 0.05 mm and 0.03 mm for points at (66.6617°S, 140.0014°E), (70.5°S, 135.5°E), and (70.5°S, 45.5°E). This is good enough for GLAS tidal loading correction.

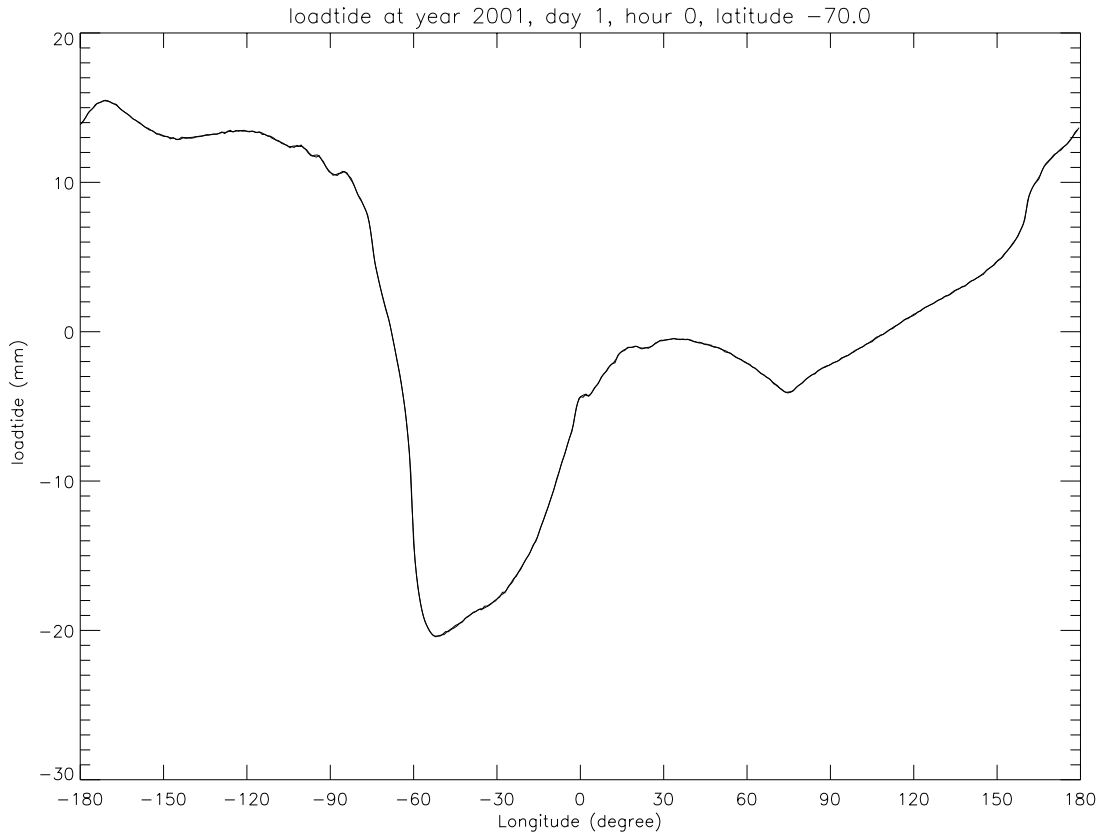


**Figure 4.** Vertical displacements at epoch 2001 00:00:00, along a small circle of latitude 70°S. Two estimates are shown, calculated at points separated by 1° and 0.5° longitude intervals, respectively. The excellent agreement justifies the practice of computing load tides on a coarse grid and interpolating bilinearly in space.

## 6. Tests of the significance of the loading correction

A typical technique used in altimetry research is crossover point analysis. This is done by comparing elevation estimates at successive passes (e.g. ascending and descending measurements) at a single location at the surface. We used a set of crossover points at high southern latitudes, provided by Dr. Schutz's group at University of Texas for an eight day repeat orbit scenario.

Figure 5 shows the tide loading effect over a crossover point at (67.7799°S, 123.1133°E) for the year 2001. Here we only consider the effect of tidal loading, in order to ascertain whether a beat pattern between tide frequencies and orbital periods might lead to aliased signals masquerading as systematic changes in elevation. Figure 5(a) shows the tidal load variation for the year 2001, starting on January 1, and calculated at one hour intervals. The apparent surface elevation



changes for ascending and descending paths at the fiducial point are shown in Figures 5(c) and 5(e). Although individual differences could reach 30 mm, the differences for both ascending and descending passes have means of about zero and standard deviations of about 8 mm (Figures 5d and 5f). This means that if a sufficient number of measurements are used in calculating the surface elevation at this location, for this mission scenario, the bias would be small (several mm). The rms error for a single measurement is found to be less than  $\pm 10$  mm. The error would be much smaller inland than along the coast.

It is difficult to assess the possibility of biases based on this single calculation. Indeed, there could be instances where the bias could be much more severe. By applying the tidal loading correction discussed above, such possible biases introduced by ocean tidal loading can be avoided. As shown above, ocean tide loading corrections are easily provided along the satellite ground tracks. Applying these corrections will improve the accuracy of satellite altimeter measured surface elevations over polar regions, especially in the near coast area where the amplitude of the load tide is larger than inland.

The histogram of these displacement values, shown in frame 5(b) shows that the distribution is significantly skewed at that location, although the mean over the 365-day cycle is very close to zero. This skewness is caused primarily by the near commensurability of the frequencies of certain tide components. (For instance, the histogram of values of the function  $\cos \omega t + \cos 2\omega t$  is skewed, extending from a minimum of -1.2 to a maximum value of +2.) Furthermore, because this commensurability is nearly perfect for components  $k_1$  and  $k_2$ , this phenomenon may persist with a beat period of many years. It should be noted that the degree of skewness is a function of time, and since it depends on the relative phases of the components, it depends also on location. If the beat period is in turn comparable to the repeat period of the sampling by GLAS, then it is possible for tidal loading signals to appear as small, but geographically coherent long term apparent changes in the average distribution of ice across the ice sheet. It is therefore important to perform this correction accurately. Table 1 shows the frequencies and amplitudes of the tides summed here at our test point, and Table 2 shows the beat periods of the most likely combinations of tides. The actual skewness and its actual geographical distribution is of course a result of the complex pattern of relative phases of all these components.

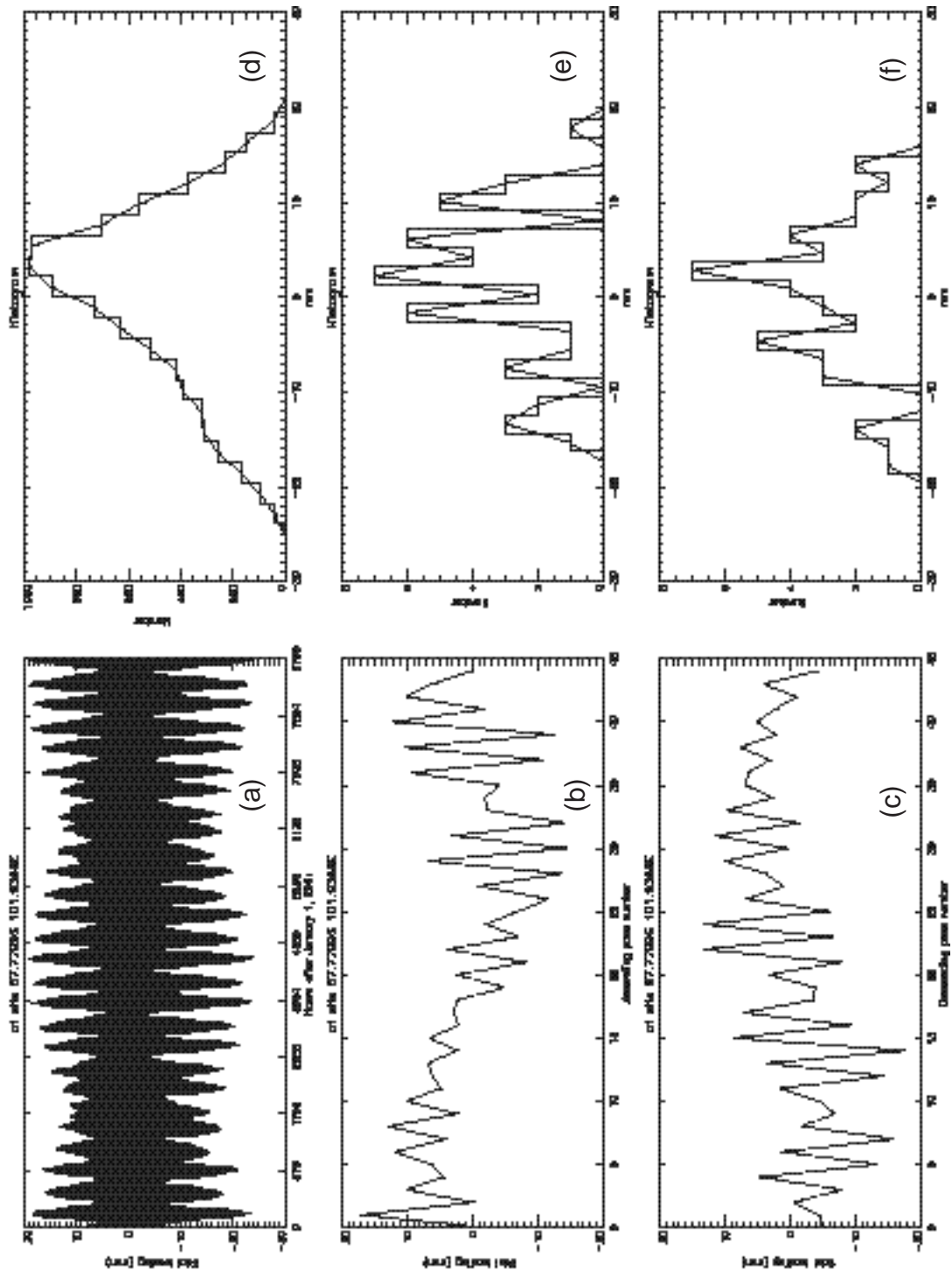


**Figure 5:** Tidal-loading variations in height and crossover analysis at 67°S, 102°E: (a) tidal-loading height variations for the year 2001; (b) surface-elevation changes at times of ascending-track passage; (c) surface-elevation changes at times of descending-track passage; (d), (e), and (f) histograms for the variations

**Table 1:** Tide frequencies and vertical displacement at location  
(67.7799°S, 101.9368°E)

Tide	Frequency (Degree/hour)	Vertical Displacement (mm)
m2	28.9841	4.7
n2	28.4397	1.4
s2	30.0000	2.0
k2	30.0821	0.8
k1	15.0411	7.9
o1	13.9430	7.2
p1	14.9589	2.4
q1	13.3987	1.4

**Table 2:** Beat frequencies of selected pairs of tidal components

Tide Pairs	Repeat Period (years)
k1 ~ k2	410.68
k2 ~ s2	0.50
p1 ~ s2	0.50
p1 ~ k2	0.25

## References

- Agnew, D. C., SPOTL: Some programs for ocean-tide loading, SIO Ref. Ser. 96-8, 35 pp., Scripps Inst. of Oceanogr., La Jolla, Calif., 1996
- Baker, T. F., Method of tidal loading computation, MAREES TERRESTRES. BULLETIN D'INFORMATIONS, Vol. 94, 6365-6373, 1985.
- Bentley, C. R. and D. D. Sheehan. Comparison of altimetry profiles over East Antarctic from Seasat and Geosat, an interim report. *Z. Gletscherkd, Glazialgeol.*, 26(1), 1-9, 1992.
- Brenner, A. C., R. A. Bindschadler, R. H. Thomas, and H. J. Zwally, Slope-induced errors in radar altimetry over continental ice sheets. *J. of Geophys. Res.*, 88(c3), 1,617-1,623, 1983.
- Doodson, A. T., The analysis of tidal observations. *Phil. Trans. Roy. Soc. Lond.*, 227, 223-279, 1928
- Eanes, R. J., Diurnal and semidiurnal tides from TOPEX/POSEIDON altimetry, *Eos Trans. AGU*, 1994 Spring Meeting Suppl., 108, 1994.
- Egbert, G. D., A. F. Bennett, and M. G. G. Foreman, TOPEX/POSEIDON tides estimated using a global inverse model, *J. Geophys. Res.*, 99, 24821-24852, 1994.
- Farrell, W. E., Deformation of the Earth by surface loads, *Rev. Geophysics and Space Phys.*, 10, 761-797, 1972.
- Haines, B. J., G. H. Born, R. C. Williamson, and C. J. Koblinsky. Application of the GEM-T2 gravity field to altimetric satellite orbit computation. *J. Geophys. Res.* 99(c8), 16,237-16,254, 1994.
- Jacobs, S. S., Is the Antarctic ice sheet growing? *Nature*, 36029-33, 1992.
- Le Provost, C., M. L. Genco, F. Lyard, P. Vincent, and P. Canceil, Spectroscopy of the world ocean tides from a finite element hydrodynamic model, *J. Geophys. Res.*, 99, 24777-24797, 1994.
- Le Provost, C., A. F. Bennett, and D. E. Cartwright, Ocean tides for and from TOPEX/POSEIDON, *Science*, 267, 639-642, 1995.
- Lingle, C. S., L. Lee, H. J. Zwally, and T. C. Seiss. Recent elevation increase on Lambert Glacier, Antarctic, from orbit crossover analysis of satellite radar altimetry. *Ann. Glacial.*, 20, 26-32, 1994.
- McCarthy, D. D. (ed), IERS Technical Note 13, 1992.
- Oerlemans, J. Possible changes in the mass balance of the Greenland and Antarctic ice sheets and their observations, projections and implications. Edited by R. A. Warrick, E. M. Barrow and T.M. L. Wigley. Cambridge University Press. 424 pp. 1993.
- Partington, K. C., W. Cudlip, and C. G. Rapley. An assessment of the capability of the satellite radar altimeter for measuring ice sheet topographic change. *Int. J. remote Sensing*, 12(3), 585-609. 1991.
- Press, W. H., S. A. Teukolsky, W. T. Vetterling, and B. P. Flannery, *Numerical Recipes in*

C. Cambridge University Press, New York, 994 pp., 1992.

Ridley, J. K. and K. C. Partington. A model of satellite radar altimeter return from ice sheets. *Int. J. Remote Sensing*. 9(4), 601-624, 1988.

Scherneck, H. G., A parameterized solid earth tide model and ocean tide loading effects for global geodetic baseline measurements, *Geophys. J. Int.*, Vol. 106, 677-694, 1991.

Schutz, B. E. Geoscience Laser Altimeter System. *MTPE/EOS Reference Handbook*. 123-134, 1995.

Schwiderski, E. W., On charting global ocean tides, *Rev. of Geophys. and Space Phys.*, Vol. 18. No. 1, 243-268, 1988.

Warrick, R. A., Climate and sea level change: a synthesis. *Climate and sea level change: Observations, projections, and implications*. Edited by R. A. Warrick, E. M. Barrow and T. M. L. Wigley. Cambridge University Press. 424 pp. 1993.

Warrick R. A. and J. Oerlemans, Sea level rise. *Climate change, the ICPP Scientific Assessment*. Edited by J. T. Houghton, G. T. Jenkins and J. J. Ephraums. Cambridge University Press. 365, pp. 1990.

Yi, D. and C. R. Bentley. A retracking algorithm for satellite radar altimetry over an ice sheet and its applications. *Glaciers, Ice Sheets, and Volcanoes: A Tribute to Mark F. Meier*. Edited by S. C. Colbeck. U.S. Army Cold Regions Research and Engineering Laboratory, Special report 96, **27**, 112-120, 1997.

Yi, D., C. R. Bentley, and M. D. Stenoien. Seasonal variation in the height of the East Antarctic ice sheet. *Ann. Glaciol.*, **24**, 191-198, 1997.

Zwally, H. J., Growth of Greenland ice sheet: interpretation. *Science*, 246(4937), 1,589-1,591, 1989.

Zwally, H. J., A. C. Brenner, J. A. Major, R. A. Bindshadler, and J. G. Marsh. Growth of Greenland ice sheet: Measurement. *Science*, 246(4937), 1,587-1,589, 1989.

Zwally, H. J., A. C. Brenner, J. A. Major, T. V. Martin and R. A. Bindshadler. Satellite radar altimetry over ice. Vol. 1, *Processing and corrections of Seasat data over Greenland*, Washington, DC, National Aeronautics and Space Administration. (NASA Ref. Pub. 1233, 1.)